Proceedings of ICFA Mini-Workshop on Impedances and Beam Instabilities in Particle Accelerators, Benevento, Italy, 18-22 September 2017, CERN Yellow Reports: Conference Proceedings, Vol. 1/2018, CERN-2018-003-CP (CERN, Geneva, 2018)

VLASOV SOLVERS AND MACROPARTICLE SIMULATIONS

N. Mounet*, CERN, Geneva, Switzerland

Abstract

We review here two essential methods to evaluate growth rates of transverse coherent instabilities arising from beam-coupling impedance in a synchrotron, namely Vlasov equation solvers and tracking simulation of macroparticles. We will discuss the basics of the two methods, reviewing in particular the theoretical grounding of Vlasov solvers – giving all the necessary formulas in the case of the DELPHI solver. We will then assess the advantages and limitations of the two methods, by showing a number of practical applications, both in hadrons machines such as the CERN LHC and SPS, and in lepton synchrotrons such as LEP. In particular, we will show how the Vlasov solver DELPHI can help understanding the relative lack of success in trying to stabilize the transverse mode coupling instability using a reactive or resistive transverse feedback in LEP.

INTRODUCTION

Beam instabilities due to self-interaction fields in synchrotrons have been a matter of concern since the early days and the pioneer works of Laslett et al [1] and of Vaccaro and Sessler [2], the latter introducing the concept of beam-coupling impedance. Such instabilities can be critical in limiting the machine performance, in particular in the transverse plane. One can mention for instance the Large Electron Positron collider (LEP) transverse mode coupling instability (TMCI) that was limiting the single-bunch current to less than 1 mA [3–7], or more recently the transverse instabilities observed in the Large Hadron Collider (LHC) during run I and II at top energy, which led to the use of very high current in the octupolar magnets (close to the maximum available) to provide enough Landau damping [8, 9].

A number of methods can be used to assess beam stability in a synchrotron and the efficiency of mitigation techniques to overcome instabilities, such as a transverse feedback system, or Landau damping from optics non-linearities. Historically, one of the first attempts to understand theoretically coherent beam instabilities was done thanks to Vlasov formalism [10], e.g. in the work of Sacherer [11]. This approach considers the phase space as a continuous medium and finds the modes that can develop upon the action of impedance, resorting to perturbation theory to solve the equation.

Another approach is to use tracking simulations in which the beam is rather looked as a collection of macroparticles which are tracked down the full ring, in an attempt to be as realistic as possible. In that case, the goal is to observe directly the time evolution of the beam transverse motion.

These two methods are currently widely used and will be the focus of these proceedings. Among the other approaches that exist, one can mention the circulant matrix model (CMM) [12–15], which discretizes the longitudinal phase space in fractions of hollow rings, building a one-turn map for each part of the distribution defined. Instability modes can be found from the diagonalization of the one-turn matrix. Also, it is worth mentioning that Vlasov equation is sometimes solved in time domain rather than in mode domain; for instance Ref. [16] does so using Lie algebraic techniques and exponential operators.

In these proceedings we will first describe the theory underlying Vlasov solvers operating in mode domain. Then the approach adopted in macroparticles tracking codes will be explained, before showing some limitations and assets of each method with the help of practical examples in the CERN LEP, LHC and SPS (Super Proton Synchrotron). Our concluding remarks will follow.

Note that in all the following we use SI units and the $e^{j\omega t}$ convention for the Fourier transform, i.e. unstable modes exhibit a tune shift with a negative imaginary part.

VLASOV SOLVERS: THEORY

Since as early as 1972, several (semi-)analytical Vlasov solvers for the transverse plane have been theorized and/or implemented. As a non-exhaustive list one can mention (in chronological order): Sacherer integral equation [11] and Sacherer analytical formulas giving complex tuneshifts [17, 18], Besnier formalism with orthogonal polynomials [19, 20], Laclare eigenvalue formalism [21], the code MOSES (MOde-coupling Single bunch instability in an Electron Storage ring) [22, 23], Chao's general formulation [24], Scott Berg's theory [25], Karliner and Popov's theory for impedance-driven instabilities with a feedback system [26], the nested head-tail Vlasov solver (NHTVS) [27], the semi-analytical code DELPHI (for Discrete Expansion over Laguerre Polynomials and Head-tail modes to compute Instabilities) [28] and the code GALACTIC (for GArnier-LAclare Coherent Transverse Instabilities Code) [29].

All these approaches have a common theoretical grounding, based on Vlasov equation [10] and the perturbation theory used to solve it in mode domain. We will provide here an an outline of the formalism, following closely the approach of Chao [24, chap. 6], and adding a few recent developments to include a bunch-by-bunch transverse feedback damper, as in Refs. [26–29].

Vlasov equation expresses the conservation of the local phase space density over time for a collection of collisionless particles (hence excluding any effect from intra-beam scattering) under the influence of external electromagnetic forces. This includes the self-interaction field from the beam-coupling impedance because it can be seen as a collective field from the ensemble of particles. The forces have to be non-dissipative, which excludes from the following treat-

* nicolas.mounet@cern.ch

https://doi.org/10.23732/CYRCP-2018-001.77

ment the effect of synchrotron radiation. Note that damping and diffusion from synchrotron radiation can be introduced using the Fokker-Planck equation [30] – see e.g. Ref. [31] for an example of Vlasov-Fokker-Planck solver in the context of storage rings and light sources.

Vlasov equation, written for the general phase space distribution density ψ, reads

$$\frac{d\psi}{dt} = 0. \quad (1)$$

Choosing the independent variable to be the longitudinal position along the accelerator orbit, $s = vt$ with v the beam longitudinal velocity and t the time, and focusing our study on the y transverse plane, we can write the single particle unperturbed 4D Hamiltonian as

$$H_0 = \frac{Q_y}{R} J_y - \frac{1}{2\eta}\left(\frac{\omega_s}{v}\right)^2 z^2 - \frac{\eta}{2}\delta^2, \quad (2)$$

with $Q_y = Q_{y0} + Q'_y \delta$ the vertical tune which includes here both the unperturbed tune Q_{y0} and the chromaticity Q'_y, R the machine physical radius, $\eta = \alpha_p - \frac{1}{\gamma^2}$ the slippage factor (α_p being the momentum compaction factor), ω_s the synchrotron angular frequency, $(z, \delta = \frac{dp}{p})$ the longitudinal phase space coordinates inside the beam, and (J_y, θ_y) the action-angle variables defined from the (y, p_y) vertical coordinate and momentum as

$$J_y = \frac{1}{2}\left(\frac{Q_{y0}}{R} y^2 + \frac{R}{Q_{y0}} p_y^2\right), \quad (3)$$

$$y = \sqrt{2J_y \frac{R}{Q_{y0}}} \cos\theta_y, \qquad p_y = \sqrt{2J_y \frac{Q_{y0}}{R}} \sin\theta_y. \quad (4)$$

Lattice non-linearities in the transverse plane are neglected at this stage (but we will see later how to include them back to treat Landau damping) and the linear coupling between the x and y planes is assumed to be zero. We consider now the effect of a transverse dipolar impedance and a transverse feedback, both in the y coordinate, hence excluding other kinds of collective effects such as direct space charge, beam-beam effects, or electron cloud. The impedance and feedback are assumed to be lumped in a single point of the circular synchrotron; this simplification can be made, provided: 1/ the instabilities are much slower than a single turn around the machine, and 2/ the impedances are weighted appropriately by the β functions ratio between their actual location and the location where the lumped impedance is applied (see e.g. Refs [32, 33]). To include the effect of both impedance and damper, we add to the unperturbed Hamiltonian a perturbation of the form

$$\Delta H = -\frac{y}{E} F_y(z, s), \quad (5)$$

where E is the total energy of a particle, and $F_y(z, s)$ the vertical force due to the impedance and/or damper, felt by a particle at a longitudinal position z inside the beam. As in Ref. [24, chap. 6], for convenience we will use the polar coordinates (r, ϕ) in the longitudinal plane, such that z and δ can be expressed as

$$z = r\cos\phi, \qquad \frac{\eta v}{\omega_s}\delta = r\sin\phi. \quad (6)$$

Neglecting the impact of chromaticity and of F_y on the longitudinal invariant [1], the unperturbed stationary distribution can be written [24, chap. 6]

$$\psi_0\left(y, p_y, z, \delta\right) = f_0(J_y) g_0(r), \quad (7)$$

with f_0 and g_0 two distribution functions. To find eigenmodes arising from the beam-coupling impedance we use perturbation theory and add to ψ_0 a perturbation of the general form [24, chap. 6]

$$\begin{aligned}\Delta\psi\left(s, y, p_y, z, \delta\right) &= e^{j\Omega s/v} f_1(J_y, \theta_y) \cdot g_1(r, \phi) \\ &= e^{j\Omega s/v} \sum_{k=-\infty}^{+\infty} f_1^k(J_y) e^{jk\theta_y} \\ &\quad \cdot e^{\frac{-jQ'_y z}{\eta R}} \sum_{l=-\infty}^{+\infty} R_l(r) e^{-jl\phi}, \end{aligned} \quad (8)$$

with $\Omega = \omega_0 Q_c$ the angular frequency of the eigenmode looked for ($\omega_0 = 2\pi f_0 = v/R$ being the angular revolution frequency and Q_c the complex tune shift of the mode), and where we have expanded both f_1 and g_1 as Fourier series. Writing Vlasov equation for the total perturbed distribution $\psi_0 + \Delta\psi$ and using the full Hamiltonian $H_0 + \Delta H$ to get the derivatives vs. s of J_y, θ_y, z and δ, one can show that all $f_1^k(J_y)$ must be zero except $f_1^{\pm 1}(J_y)$, and that $f^1(J_y)$ is negligible provided Q_c is close to Q_{y0} (which is a very robust assumption). Defining $f(J_y) \equiv f^{-1}(J_y)$ and $\omega_s = \omega_0 Q_s$ we get

$$\begin{aligned}\sum_{l=-\infty}^{+\infty} R_l(r) \left[\frac{f(J_y)(Q_c - Q_{y0} - lQ_s)}{f'_0(J_y)\sqrt{\frac{2J_y R}{Q_{y0}}}}\right] e^{-jl\phi} &= \\ \frac{Re^{-j\frac{Q_c s}{R}}}{2E} F_y(z, s) e^{\frac{jQ'_y z}{\eta R}}&, \end{aligned} \quad (9)$$

which means that the term between square brackets is constant, and

$$f(J_y) = D f'_0(J_y)\sqrt{\frac{2J_y R}{Q_{y0}}}, \quad (10)$$

with D proportional to the dipolar moment of the beam. The remaining unknowns are the radial functions $R_l(r)$.

After expressing the force $F_y(z, s)$ from the combined effect of the dipolar impedance $Z_y(\omega)$ and of the transverse bunch-by-bunch damper of damping time n_d turns (which can be seen as a purely imaginary wake function of constant

[1] This makes the system slightly non Hamiltonian in principle, but the corresponding terms can be neglected when the system remains far from synchro-betatron resonances, and as long as the transverse beam size remains small [24, chap. 6].

amplitude, i.e. a delta function in frequency domain), in terms of the $R_l(r)$, and plugging the resulting expression into Vlasov equation, one can get the following extension of Sacherer integral equation [11]:

$$(\Omega - Q_{y0}\omega_0 - l\omega_s)R_l(\tau) = -\kappa g_0(\tau) \sum_{l'=-\infty}^{+\infty} j^{l'-l} \cdot \int_0^{+\infty} \tau' R_{l'}(\tau') \left[\mu J_l\left(-\omega_\xi \tau\right) J_{l'}\left(-\omega_\xi \tau'\right) \mathrm{d}\tau' + \sum_{p=-\infty}^{+\infty} Z_y(\omega_p) J_l\left((\omega_\xi - \omega_p)\tau\right) J_{l'}\left((\omega_\xi - \omega_p)\tau'\right)\right], \tag{11}$$

with J_l the Bessel functions and[2]

$$\omega_\xi = \frac{Q'_y\omega_0}{\eta}, \qquad \omega_p = (n + pM + [Q_{y0}])\omega_0, \qquad \kappa = -j\frac{Nf_0e^2M}{2\gamma m_0 c Q_{y0}}, \qquad \tau = \frac{r}{v}, \qquad -\kappa\mu = j\frac{\omega_0}{n_d}, \tag{12}$$

where N is the number of particles per bunch, γ the relativistic mass factor, m_0 the particles mass, e the elementary charge, $[Q_{y0}]$ the fractional part of the tune, M the number of bunches and n the coupled-bunch mode number (between 0 and $M - 1$).

In most of the aforementioned codes and theories, Sacherer integral equation ultimately translates into an eigenvalue problem by either

- expanding the radial functions $R_l(\tau)$ over a complete basis set (typically orthogonal polynomials such as Laguerre polynomials as e.g. in the codes MOSES [22, 23], DELPHI [28] and the approach of Karliner and Popov [26], or Jacobi polynomials in Besnier's method [20]),
- considering a specific, easy to solve, longitudinal distribution, e.g. the airbag distribution (this case can be solved almost fully analytically [24, chap. 6]), or a superposition of such airbag distributions [27],
- solving the equation in frequency domain, i.e. by considering as the unknown the amplitude of the spectrum at ω_p of the signal observed at a pickup:

$$\sigma_l(p) \propto \int_0^{+\infty} J_l\left((\omega_p - \omega_\xi)\tau\right) R_l(\tau)\tau\mathrm{d}\tau, \tag{13}$$

as done in Laclare's formalism [21] and in GALACTIC [29].

[2] The normalization of the damper gain is set in such a way that when $Z_y = 0$ and $Q'_y = 0$, one should get a purely imaginary frequency shift equal to $j\frac{f_0}{n_d}$ (corresponding to a damping time of n_d turns). Under these assumptions the right hand side of Eq. (11) is non zero only for $l = 0$, and only the term $l' = 0$ remains in the sum. Multiplying Eq. (11) by τ, integrating from 0 to $+\infty$, and knowing that $\int_0^{+\infty} \mathrm{d}\tau\tau g_0(\tau) = \frac{1}{2\pi}$, one then gets the normalization equality $-\kappa\mu = j\frac{\omega_0}{n_d}$.

In any case one ends up with an eigenvalue problem of the general form

$$(\Omega - Q_{y0}\omega_0)\alpha_{ln} = \sum_{l'=-\infty}^{+\infty}\sum_{n'=0}^{+\infty} \alpha_{l'n'}\left(\delta_{ll'}\delta_{nn'}l\omega_s + \mathcal{M}_{ln,l'n'}\right), \tag{14}$$

where the α_{ln} coefficients represent the eigenmode looked for, δ_{lk} is the Kronecker delta, and $\mathcal{M}_{ln,l'n'}$ is an infinite matrix extending over respectively radial and azimuthal mode numbers l and n. The eigenvalues provide the coherent mode frequency shifts, among which the most unstable ones can be easily spotted by looking at their imaginary part. To solve the problem numerically, the matrix has to be truncated, and the convergence of the truncation has in principle to be checked. In the Appendix we describe how the final eigenvalue problem is obtained and solved in the case of the DELPHI code.

Note that the problem can be simplified even further by considering only a single azimuthal mode at a time, as in e.g. the low-intensity version of Laclare's approach.

Each of the methods described above has its assets and drawbacks: the approaches using an expansion over orthogonal polynomials are very general as they can be used with any impedance and any longitudinal distribution, but they end-up with matrix coefficients involving a weighted sum of impedance terms taken at an infinite number of betatron sidebands, the calculation of which might be computationally intensive; the airbag methods are very efficient but assume a certain shape for the longitudinal distribution; and Laclare's approach gives rise to easy-to-compute matrix elements, but these explore only a finite frequency domain, such that a smooth impedance might require a very large matrix size to get reliable results.

Note that in the widely used Sacherer's approach [17], the problem is simplified even further by assuming *a priori* a given functional form for the radial functions $R_l(\tau)$ (or equivalently, of the spectrum amplitude $\sigma_l(p)$) and computing the right hand side of Eq. (11) to get the complex frequency shifts.

Finally, Landau damping from amplitude detuning due to lattice non-linearities, can be introduced in several ways:

- using the stability diagram theory: first the coherent frequency shifts are obtained by solving the eigenvalue problem (14) without considering any tunespread; then the stability is checked *a posteriori* by comparing the complex frequency shifts obtained to the stability region calculated using dispersion integrals of the unperturbed transverse distribution [1, 18, 34–37],
- including the tunespread in Vlasov equation from the beginning when computing the coherent modes, as done in e.g. Refs. [28, 38]. Rather than an eigenvalue problem of the form (14), one then has to solve a more general, non-linear equation to get the complex coher-

ent tuneshift $Q_c = \frac{\Omega}{\omega_0}$:

$$\det\left(\left[\delta_{ll'}\delta_{nn'}\frac{\omega_0}{I_l(Q_c)}\right] + \left[\mathcal{M}_{ln,l'n'}\right]\right) = 0, \qquad (15)$$

with the dispersion integrals $I_l(Q_c)$ given by (considering here the octupoles as the only source of detuning)

$$I_l(Q_c) = \iint_0^{+\infty} \frac{\frac{\partial f_0(J_x,J_y)}{\partial J_y} J_y \mathrm{d}J_x \mathrm{d}J_y}{Q_c - Q_{y0} - a_{yy}J_y - a_{yx}J_x - lQ_s}, \qquad (16)$$

where a_{yy} and a_{yx} are the detuning coefficients from the octupoles, and where for clarity we have reintroduced the dependency on the horizontal action J_x of the transverse unperturbed distribution f_0.

THE MACROPARTICLE TRACKING APPROACH

One of the most reliable ways to assess beam stability in a machine is to run time domain macroparticles tracking simulations. A number of codes are able to deal with impedance effects, among which one can mention HEADTAIL [39–41] and PyHEADTAIL [42, 43] (with the inclusion of electron-cloud effects), ORBIT [44] and PyORBIT [45] (where the direct space-charge forces are also included), MTRISM [46] (for coupled-bunch instabilities), MUSIC [47] (with an optimized algorithm for wake functions given by a sum of resonators), BEAMBEAM3D [14, 48] and COMBI [14, 49] (with the inclusion of beam-beam effects), SBTRACK and MBTRACK [50–53] (for storage rings and light sources).

In e.g. the HEADTAIL and PyHEADTAIL codes, the bunches are sliced longitudinally; slices contain a number of macroparticles, each representing a fraction of the bunch charge – typically there are much less macroparticles than actual particles in the bunch, but enough to get a good representation of the phase space. Each individual macroparticle i is tracked through the ring which is subdivided into one or several sections, and essentially goes through two steps per section: 1) wake fields kicks are applied, and 2) its transverse phase space coordinates are linearly transported to the next section. In addition, once per turn the synchrotron motion is applied to the longitudinal coordinates.

The kicks due to impedance $\Delta x_i'$, $\Delta y_i'$ and $\Delta\delta_i$ are computed straightforwardly using the time domain counterparts of the impedances, namely the longitudinal, horizontal and vertical wake functions $W_{||}$, W_x and W_y respectively:

$$\begin{aligned}
\Delta x_i' &= C \sum_{z_S > z_{S_i}} n_S W_x\left(z_{S_i} - z_S, x_S, y_S, x_{S_i}, y_{S_i}\right), \\
\Delta y_i' &= C \sum_{z_S > z_{S_i}} n_S W_y\left(z_{S_i} - z_S, x_S, y_S, x_{S_i}, y_{S_i}\right), \\
\Delta\delta_i &= -C \sum_{z_S \geq z_{S_i}} n_S W_{||}\left(z_{S_i} - z_S\right), \qquad (17)
\end{aligned}$$

where $C = \frac{e^2}{E_0\beta^2\gamma}$, $\beta = \sqrt{1-\gamma^{-2}}$, E_0 is the rest mass of the elementary particles (protons, electrons or ions) and e the elementary charge. S_i is the slice containing the macroparticle i, and n_S, x_S, y_S, z_S are resp. the number of particles, transverse positions and longitudinal position, of each slice S (z decreases when going toward the tail of the bunches)[3]. The slices S are used here only for the computation of the convolution of the wake functions with the bunch profile, and the slicing has to be fine enough for the features of the wake functions to be taken into account appropriately, as well as to allow the proper modes to develop. Tunespread (and therefore Landau damping) from external non-linearities is taken into account in a straightforward manner, by simply computing the transport properties of each macroparticle as a function of its phase space coordinates – this works equally well in the transverse and longitudinal planes. Wake functions can include several terms, e.g. W_x is in general given by

$$\begin{aligned}
W_x(z, x_S, y_S, x_{S_i}, y_{S_i}) &= W_x^{dip}(z)x_S + W_{xy}^{dip}(z)y_S \\
&+ W_x^{quad}(z)x_{S_i} + W_{xy}^{quad}(z)y_{S_i}, \qquad (18)
\end{aligned}$$

where dip stands for "dipolar" and $quad$ for "quadrupolar" (coupled terms – i.e. wakes in the x direction but proportional to the y position and vice versa – being also taken into account). Depending how far the code goes in the wake sums, multiturn effects are included.

Most of the codes mentioned above rely on a similar slicing to compute the effect of impedance, at the notable exceptions of ORBIT [44] and MUSIC [47] which have implemented optimized ways to take into account specific impedances such as those given by a superposition of resonators.

We should finally stress that the usefulness of most codes depend on the availability of post-processing tools able to make their outputs human-readable and/or comparable to real machine data. Examples of applications where such post-processing tools are used, can be found in the references quoted above.

PRACTICAL EXAMPLES AND COMPARISON BETWEEN THE TWO APPROACHES

Vlasov solvers and macroparticle simulations, when applied on the same situation and when both are well converged, give the same result, as they are just two different ways to solve the same problem. One striking example is the benchmark obtained between the MOSES Vlasov solver and HEADTAIL in Ref. [54], which is reproduced in Fig. 1. In this plot the coherent motion simulated with HEADTAIL was post-processed with SUSSIX [55] and displayed using white dots, whose size and brightness are both non-linear functions of their spectral amplitude (large bright dots have a higher amplitude than small dark dots).

[3] In the above expressions the sums run over all slices and bunches before the slice of the macroparticle considered, which is correct only for $\beta = 1$. Actually, in PyHEADTAIL the implementation is more general and for low energy machines the "wake in front" can be included as well.

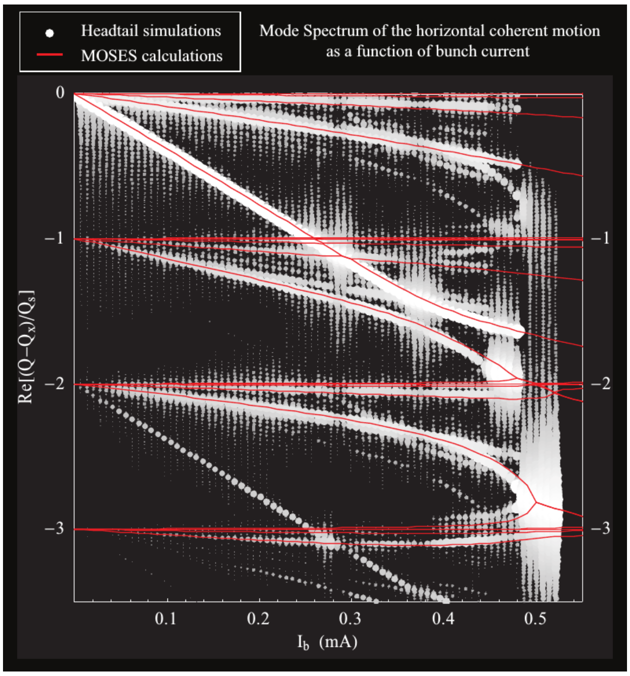

Figure 1: Comparison between HEADTAIL (white dots) and MOSES (red lines) mode spectra, as a function of bunch intensity, in the case of the SPS at injection energy ($p = 26$ GeV$/c$), with a broadband resonator impedance of 10 MΩ/m (cutoff frequency 1 GHz, quality factor $Q = 1$), zero chromaticity, $Q_s = 3.24 \cdot 10^{-3}$, $Q_x = 26.185$, r.m.s. bunch length $\sigma_z = 21$ cm and r.m.s. momentum spread $\sigma_\delta = 9.3 \cdot 10^{-4}$. Courtesy B. Salvant [54].

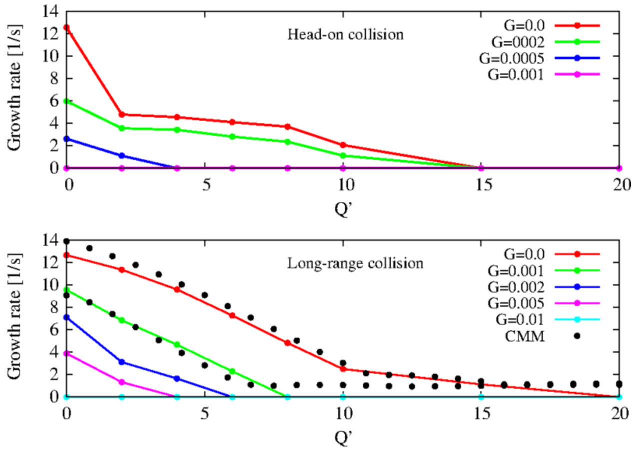

Figure 2: Instability growth rate as function of damper gain $1/n_d$ (with n_d defined in Eq. (12)) and chromaticity for long-range (bottom) and head-on (top) single-bunch collision in the LHC, obtained with the BEAMBEAM3D code [48], in a situation where the beam-beam tune shift is adjusted to be at the location of a mode coupling instability between coherent beam-beam dipole modes and high order headtail modes. The black dots are from calculations using the circulant matrix model (CMM) [13, 15]. Courtesy S. White *et al* [14].

Macroparticle simulations, nevertheless, can assess stability in complex, realistic situations, typically out of reach to a Vlasov solver, for instance: localized impedance sources (going beyond the lumped impedance approximation), any kind of feedback damper, synchrotron radiation damping, and even the combination of impedance with other collective effects such as space-charge, electron cloud, or beam-beam. As an example we show in Fig. 2, extracted from Ref. [14], the growth rate of a strong mode arising from the coupling between impedance and beam-beam effects, as a function of chromaticity, damper gain and with either long-range separation (10σ, where σ is the RMS transverse beam size) or head-on collisions. This illustrates the potential of the macroparticle tracking approach: in this case it is able to evaluate the combined effect of impedance, damper, chromaticity, and beam-beam interactions in the strong-strong regime, which all together involves such mechanisms as high order headtail instabilities, mode coupling, non-linearities and Landau damping.

This kind of "brute force" simulation approach is very useful and can provide both a complete vision of the problem studied and accurate answers – if the impedance model is precise enough. Yet, if many sophisticated machine and beam features can be included almost at will in such tools, one obvious drawback is that they can be very computationally intensive, limiting their usability, for instance, in cases where the combined effect of coupled-bunch and intra bunch motion has to be evaluated, for slow instabilities, or for those requiring a large latency time to develop. Also, the interpretation of simulation results can be tricky when it comes to understand the mechanism underlying the instabilities observed.

More fundamentally, as a time domain tool such simulations are essentially unable to predict what happens after an infinite time, hence a difficulty when it comes to state that a given configuration is stable. To illustrate this point, we show in Fig. 3 the result of HEADTAIL simulations for a single bunch in the LHC, with various octupole currents. While the effect of Landau damping is clearly observed with increasing non-linearities, the stability threshold is uneasy to determine: for instance, with 130A the beam seems more unstable than with 120A, and it remains unclear if the beam is really stable even at 150A or is going to become unstable if we simulate more turns. Conversely, had we stopped the simulation of the 110A case at 10^5 turns we would have probably concluded that the beam is stable, while it is not if we go further in the simulation.

On the other hand, slow instabilities are usually not a problem for Vlasov solvers, because they operate in "mode domain" such that any unstable mode, being slow or fast, will be spotted. They are also typically much less computationally intensive than macroparticle simulations, at least when they are based on (semi-)analytical formulas. This comes at the price of having a range of applicability less broad than macroparticle tracking. Moreover, any additional ingredient to be put in such a solver typically requires pages of analytical derivations; for example adding the Q'' term in the theory presented in the first section (and doing so

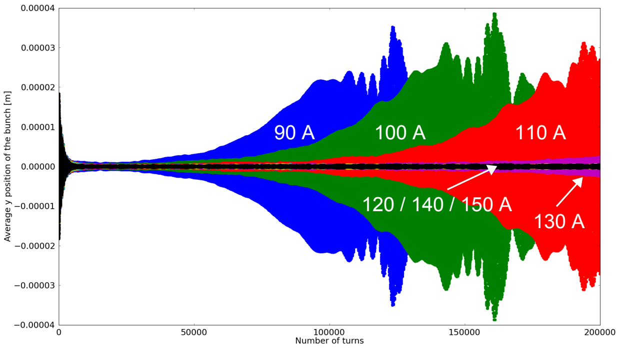

Figure 3: Vertical centroid motion vs. number of turns from HEADTAIL simulations, for a single bunch in the LHC at 4TeV$/c$, Q'_y=6, with respectively 2.5eV.s and 2mm.mrad of longitudinal and normalized vertical emittances, $N = 1.7 \cdot 10^{11}$ protons, and various octupole currents. Both the amplitude detuning and the second order chromaticity Q'' due to the octupoles are included in the simulations. We use the LHC impedance model from Ref. [56].

without the stability diagram approximation), is much more difficult than adding the corresponding term in the detuning of a macroparticle tracked in HEADTAIL.

Still, the mode approach sometimes helps to get a better understanding of instabilities, so can complement advantageously and ease the interpretation of more realistic simulations. Moreover, the rapidity of the computations in conjunction with the fact that the matrix diagonalized can be re-used for different intensities or damper gain (see Eqs. (14) and (21)) gives the ability to perform large parameter scans, and therefore to get a better global view of the stability of a given machine. To illustrate this point, we re-investigate here the case of LEP transverse mode-coupling instability (TMCI) and try to explain the relative lack of success in the various attempts to stabilize it with a transverse bunch-by-bunch feedback [7]. Over the years of operation of LEP, at least two kinds of damper were tested: a reactive feedback, to prevent the azimuthal mode 0 to shift down and couple with the azimuthal mode -1 [12, 57, 58], and a resistive feedback, which was tried at LEP but never used in operation, and thought to be a good option by Karliner-Popov [26] five years after the LEP closure. It is also worth mentioning that there was in general a good agreement between measurements of the TMCI threshold (just below 1 mA) and the LEP impedance model [7].

To try to explain these observations, we show in Figs. 4 and 5 two-dimensional plots where the color represents the LEP transverse instability threshold[4], obtained using the DELPHI Vlasov solver, as a function of the chromaticity and feedback gain, for respectively a resistive and a reactive feedback. It appears clearly that the resistive feedback does not improve the instability threshold, and the reactive one can improve it only marginally (at high feedback gain). This is in qualitative agreement with the observations in LEP.

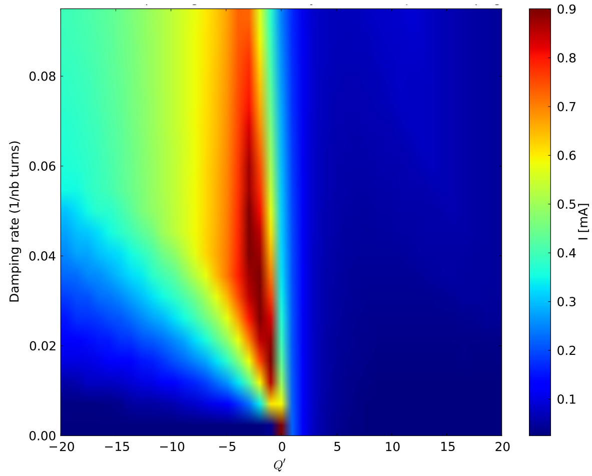

Figure 4: Transverse instability threshold (color) vs. chromaticity and damper gain of a transverse resistive feedback, from DELPHI, in LEP at 22 GeV, r.m.s. bunch length 1.3 cm, circumference 26.659 km, $Q_x = 76.194$, $Q_s = 0.108$ and $\alpha_p = 1.855 \cdot 10^{-4}$. The impedance model contains two broad-band resonators for the RF cavities and the bellows, of shunt impedances resp. 1.1 and 0.23 MΩ/m, cutoff frequencies resp. 2 and 12 GHz, and quality factors $Q = 1$. The instability threshold is defined as the intensity at which the growth rate exceeds the synchrotron damping rate.

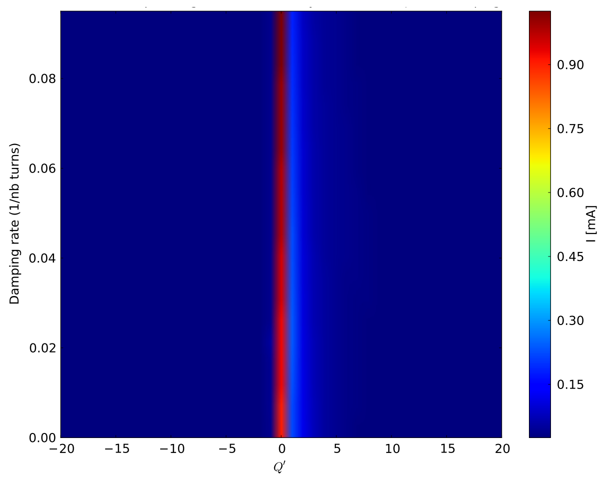

Figure 5: Transverse instability threshold (color) in LEP vs. chromaticity and damper gain of a transverse reactive feedback, from DELPHI. Parameters are the same as in Fig. 4.

CONCLUSION

In these proceedings we outlined the theoretical basis and assumptions behind typical Vlasov solvers, giving an

[4] Strictly speaking, the instability threshold here represents the TMCI threshold only at zero chromaticity; when the chromaticity deviates from zero, headtail instabilities may occur before the TMCI threshold is reached.

extended version of Sacherer integral equation in the case when a bunch-by-bunch damper is present. The general structure of the final eigenvalue problem was shown and the various strategies to solve it summarized. Explicit details and formulas were given in the case of the DELPHI code.

We also described the practical approach adopted in many macroparticle codes to simulate the effect of impedances. Comparing the two approaches through a few specific examples, we showed that Vlasov solvers and macroparticle simulations are two equivalent ways to predict coherent instabilities; they give essentially the same results when they can be applied to the same situation. On the other hand they differ a lot in their range of applicability, flexibility and speed.

While macroparticle simulation codes are simple in essence, so easily extensible, Vlasov solvers typically require complete re-derivations of complex analytical formulas when any ingredient has to be added. Macroparticle simulations can deal with very complex beam and machine configurations, and hence can be very computationally intensive, when Vlasov solvers are typically much faster, at the expense of having to be used in simplified and idealized situations. Still, macroparticle simulations are fundamentally unable to guess what happens after an infinite time, while Vlasov solvers, on the contrary, can spot even very slow growing modes.

The power of Vlasov solvers relies in the fact they can be used to make broad parameter scans; in that respect we used DELPHI to shed some light on the relative lack of efficiency of the feedback system to damp the TMCI in LEP, by showing the stability situation over a full range of chromaticities and damper gains.

ACKNOWLEDGMENT

The author warmly thanks Nicolo Biancacci, Xavier Buffat, Alexey Burov, Kevin Li, Elias Métral, Adrian Oeftiger, Giovanni Rumolo and Simon White for numerous useful discussions on the subject.

APPENDIX

Resolution of Sacherer Integral Equation in the DELPHI Code

In the codes DELPHI [28], MOSES [22] and in Karliner and Popov's approach [26], one expands the radial functions R_l over the (generalized) Laguerre polynomials $L_n^l(x) \equiv \frac{e^x x^{-l}}{n!}\frac{d^n}{dx^n}\left(e^{-x}x^{n+l}\right)$ to solve Sacherer integral equation (11):

$$R_l(\tau) = \left(\frac{\tau}{\tau_b}\right)^{|l|} e^{-a\tau^2}\sum_{n=0}^{+\infty} c_l^n L_n^{|l|}(a\tau^2), \tag{19}$$

where τ_b is the total bunch length in seconds, a an arbitrary (fixed) parameter and c_l^n the coefficients of the expansion.

The unperturbed longitudinal distribution is also expanded over Laguerre polynomials

$$g_0(\tau) = e^{-a\tau^2}\sum_{k=0}^{n_0} g^k L_k^0(a\tau^2), \tag{20}$$

with g^k the expansion coefficients. Note that the first coefficient is fully defined by the normalization condition $\int_0^{+\infty} \mathrm{d}\tau\tau g_0(\tau) = \frac{1}{2\pi}$, giving $g^0 = \frac{a}{\pi}$. The expansion (20) is performed initially and is truncated in order to get an accurate enough description of $g_0(\tau)$ - it is even exact and contains only one term in the case of a Gaussian distribution. On the other hand, truncation of the expansion of R_l in Eq. (19) sets the number of radial modes considered, and its accuracy has to be checked "on the fly" while the algorithm looks from eigenvalues. Using these decompositions, Sacherer integral equation (11) can be cast into an eigenvalue problem of the form (14) with

$$\mathcal{M}_{ln,l'n'} = \frac{-j^{l'-l}n!\kappa\tau_b^{|l|-|l'|}}{2^{|l|}(n+|l|)!}\Big[\mu G_{ln}(-\omega_\xi, a) I_{l'n'}(-\omega_\xi, a) + \sum_{p=-\infty}^{+\infty} Z_y(\omega_p) G_{ln}\left(\omega_p - \omega_\xi\right) I_{l'n'}\left(\omega_p - \omega_\xi, a\right)\Big], \tag{21}$$

using the two following integrals [59]

$$\begin{aligned} G_{ln}(\omega, a) &= (2a)^{|l|+1}\int_0^{+\infty} \tau^{1+|l|} L_n^{|l|}(a\tau^2) g_0(\tau) J_l(\omega\tau)\mathrm{d}\tau \\ &= (\omega\cdot \mathrm{sign}(l))^{|l|}\, e^{-\frac{\omega^2}{4a}} \\ &\cdot \sum_{k=0}^{n_0} g^k\,(-1)^{n+k}\, L_n^{k-n}\left(\frac{\omega^2}{4a}\right) L_k^{n+|l|-k}\left(\frac{\omega^2}{4a}\right), \end{aligned} \tag{22}$$

and

$$\begin{aligned} I_{ln}(\omega, a) &= \int_0^{+\infty} \tau^{1+|l|} L_n^{|l|}(a\tau^2) e^{-a\tau^2} J_l(\omega\tau)\mathrm{d}\tau \\ &= \frac{\mathrm{sign}(l)^{|l|}}{2a^{|l|+n+1}n!}\left(\frac{\omega}{2}\right)^{2n+|l|} e^{\frac{-\omega^2}{4a}}. \end{aligned} \tag{23}$$

In all the above, a is a fixed parameter on which one can play to optimize the algorithm, depending on the longitudinal distribution. For instance, for Gaussian longitudinal distributions we set it to $a = \frac{8}{\tau_b^2}$.

Convergence with matrix size is checked automatically by a loop which iterates the three following steps:

1. fix a number of azimuthal and radial modes, in order to truncate the matrix $\mathcal{M}$ to a finite size,
2. compute all the elements of the matrix,
3. compute its eigenvalues. If the most unstable eigenvalue(s) (i.e. those with the highest growth rate) are converged (i.e. close enough to the values obtained in the previous iteration), the algorithm stops, otherwise we go back to the first step, increasing the number of radial and azimuthal modes.

The code DELPHI can be downloaded from Ref. [60].

REFERENCES

[1] L. J. Laslett, V. K. Neil, and A. M. Sessler, "Transverse resistive instabilities of intense coasting beams in particle accelerators," *Rev. Sci. Instrum.*, vol. 36, pp. 436–448, 4 1965.

[2] A. M. Sessler and V. G. Vaccaro, *Longitudinal instabilities of azimuthally uniform beams in circular vacuum chambers with walls of arbitrary electrical properties*, CERN ISR-RF/67-2, 1967.

[3] D. Brandt, K. Hübner, and S. Myers, *On LEP performance limits in 1999 and 2000*, CERN/SL/98-005, 1998.

[4] D. Brandt and S. Myers, *LEP performance limits re-visited*, CERN/SL/98-074 DI, 1998.

[5] D. Brandt, H. Burkhardt, M. Lamont, S. Myers, and J. Wenninger, "Accelerator physics at LEP," *Rep. Prog. Phys.*, vol. 63, no. 6, pp. 939–1000, 2000.

[6] D. Brandt *et al.*, "Measurements of impedance distributions and instability thresholds in LEP," in *Proceedings of PAC'95, Dallas, Texas, USA*, 1995, pp. 570–572.

[7] J. M. Jowett, *Beam dynamics at LEP*, CERN/SL/98-029 (AP), 1998.

[8] E. Métral *et al.*, *Summary of the 2-day internal review of LHC performance limitations (linked to transverse collective effects) during run I (CERN, 25-26/09/2013)*, CERN-ACC-NOTE-2014-0006, 2014.

[9] E. Métral *et al.*, *Summary of the half-day internal review of lhc performance limitations (linked to transverse collective effects) during run II (CERN, 29/11/2016)*, CERN-ACC-NOTE-2017-0005, 2017.

[10] A. A. Vlasov, "On the kinetic theory of an assembly of particles with collective interaction," *Russ. Phys. J.*, vol. 9, pp. 25–40, 1945.

[11] F. J. Sacherer, *Methods for computing bunched-beam instabilities*, CERN/SI-BR/72-5, 1972.

[12] V. V. Danilov and E. A. Perevedentsev, *Feedback system for elimination of the transverse mode coupling instability*, CERN/SL/93-38, 1993.

[13] ——, "Feedback system for elimination of the transverse mode coupling instability," *Nucl. Instr. Meth. in Phys. Res. A*, vol. 391, 1997.

[14] S. White, X. Buffat, N. Mounet, and T. Pieloni, "Transverse mode coupling instability of colliding beams," *Phys. Rev. ST Accel. Beams*, vol. 17, no. 041002, 2014.

[15] X. Buffat, "Transverse beams stability studies at the Large Hadron Collider," PhD thesis 6321, EPFL, 2015.

[16] G. Dattoli, M. Migliorati, and A. Schiavi, "Study of coherent synchrotron radiation effects by means of a new simulation code based on the non-linear extension of the operator splitting method," *Nucl. Instr. Meth. in Phys. Res. A*, vol. 574, pp. 244–250, 2007.

[17] F. J. Sacherer, "Transverse bunched beam instabilitites - theory," in *9th International Conference on High Energy Accelerators, Stanford, California, USA*, 1974, pp. 347–351.

[18] B. Zotter and F. J. Sacherer, "Transverse instabilities of relativistic particle beams in accelerators and storage rings," in *1st International School of Particle Accelerators "Ettore Majorana"*, M. H. Blewett, Ed., CERN, Nov. 1976, pp. 175–218.

[19] G. Besnier, "Stabilitité des oscillations longitudinales d'un faisceau groupé se propageant dans une chambre à vide d'impédance réactive," *Nucl. Instr. Meth.*, vol. 164, pp. 235–245, 1979.

[20] G. Besnier, D. Brandt, and B. Zotter, *The transverse mode coupling instability in a large storage ring*, CERN LEP-TH/84-11, LHC Note 17, 1985.

[21] J. L. Laclare, "Bunched beam coherent instabilities," in *CAS - CERN Accelerator School : Accelerator Physics, Oxford, UK, 16 - 27 Sep 1985*, S. Turner, Ed., CERN, 1987, pp. 264–326.

[22] Y.-H. Chin, *Transverse mode coupling instabilities in the SPS*, CERN/SPS/85-2, 1985.

[23] ——, *User's guide for new MOSES version 2.0*, CERN/LEP-TH/88-05, 1988.

[24] A. W. Chao, *Physics of Collective Beams Instabilities in High Energy Accelerators*. John Wiley and Sons, 1993.

[25] J. Scott Berg, "Coherent modes for multiple non-rigid bunches in a storage ring," PhD thesis SLAC-R-478, Stanford Univ., 1996.

[26] M. Karliner and K. Popov, "Theory of a feedback to cure transverse mode coupling instability," *Nucl. Instr. Meth. in Phys. Res. A*, vol. 537, pp. 481–500, 2005.

[27] A. V. Burov, "Nested head-tail Vlasov solver," *Phys. Rev. ST Accel. Beams*, vol. 17, no. 021007, 2014.

[28] N. Mounet, *DELPHI: An analytic Vlasov solver for impedance-driven modes*, CERN-ACC-SLIDES-2014-0066, 2014.

[29] E. Métral, D. Amorim, S. Antipov, N. Biancacci, X. Buffat, and K. Li, "Destabilising effect of the LHC transverse damper," in *Proceedings of IPAC'18, Vancouver, Canada*, 2018, pp. 3076–3079.

[30] S. Chandrasekhar, "Stochastic problems in physics and astronomy," *Rev. Mod. Phys.*, vol. 15, pp. 1–89, 1 1943.

[31] R. L. Warnock, "Study of bunch instabilities by the nonlinear Vlasov–Fokker–Planck equation," *Nucl. Instr. Meth. in Phys. Res. A*, vol. 561, pp. 186–194, 2006.

[32] Y.-H. Chin, *Coherent synchro-betatron resonances driven by localized wake fields*, CERN/SPS/85-33, 1985.

[33] P. B. Wilson and L. Rivkin, *Threshold current for the transverse instability in PEP*, SLAC, PEP-NOTE-374, 1982.

[34] K. Hübner, A. G. Ruggiero, and V. G. Vaccaro, *Stability of the coherent transverse motion of a coasting beam for realistic distribution functions and any given coupling with its environment*, CERN ISR-TH-RF/69-33, 1969.

[35] K. Hübner and V. G. Vaccaro, *Dispersion relations and stability of coasting particle beams*, CERN ISR-TH/70-44, 1970.

[36] J. Scott Berg and F. Ruggiero, *Landau damping with two-dimensional betatron tune spread*, CERN SL-AP-96-71, 1996.

[37] E. Métral and A. Verdier, *Stability diagram for landau damping with a beam collimated at an arbitrary number of sigmas*, CERN-AB-2004-019-ABP, 2004.

[38] Y.-H. Chin, *Hamiltonian formulation for transverse bunched beam instabilities in the presence of betatron tunespread*, CERN/SPS/85-09, 1985.

[39] G. Rumolo and F. Zimmermann, "Electron cloud simulations: Beam instabilities and wakefields," *Phys. Rev. ST Accel. Beams*, vol. 5, no. 121002, 2002.

[40] G. Rumolo and E. Métral, "Simulations of single bunch collective effects using HEADTAIL," in *Proceedings of ICAP'06, Chamonix, France*, 2006, pp. 59–64.

[41] N. Mounet, E. Métral, and G. Rumolo, "Simulation of multibunch instabilities with the HEADTAIL code," in *Proceedings of ICAP'12, Rostock-Warnemünde, Germany*, 2012, pp. 262–266.

[42] K. S. B. Li *et al.*, "Code development for collective effects," in *Proceedings of ICFA Advanced Beam Dynamics Workshop on High-Intensity and High-Brightness Hadron Beams (HB'16), Malmö, Sweden*, 2016, pp. 362–367.

[43] E. Métral *et al.*, "Beam instabilities in hadron synchrotrons," *IEEE Transactions on Nuclear Science*, vol. 63, no. 2, pp. 1001–1050, 2016.

[44] A. Shishlo *et al.*, "The ORBIT simulation code: Benchmarking and applications," in *Proceedings of ICAP'06, Chamonix, France*, 2006.

[45] A. Shishlo, S. Cousineau, J. Holmes, and T. Gorlov, "The particle accelerator simulation code PyORBIT," *Procedia Computer Science*, vol. 51, pp. 1272–1281, 2015, International Conference On Computational Science, ICCS 2015.

[46] A. Koschik, "Simulation of transverse multi-bunch instabilities of proton beams in LHC," PhD thesis, Tech. Univ. Graz, 2004.

[47] M. Migliorati and L. Palumbo, "Multibunch and multiparticle simulation code with an alternative approach to wakefield effects," *Phys. Rev. ST Accel. Beams*, vol. 18, p. 031 001, 3 2015.

[48] J. Qiang, M. A. Furman, R. D. Ryne, W. Fischer, and K. Ohmi, "Recent advances of strong–strong beam–beam simulation," *Nucl. Instr. Meth. in Phys. Res. A*, vol. 558, pp. 351–355, 2006.

[49] T. Pieloni, "A study of beam-beam effects in hadron colliders with a large number of bunches," PhD thesis 4211, EPFL, 2008.

[50] R. Nagaoka, "Instability studies using evaluated wake fields and comparison with observations at SOLEIL," in *Proceedings of EPAC'06, Edinburgh, Scotland*, 2006, pp. 2847–2849.

[51] R. Nagaoka *et al.*, "Beam instability observations and analysis at SOLEIL," in *Proceedings of PAC'07, Albuquerque, New Mexico, USA*, 2007, pp. 2019–2021.

[52] R. Nagaoka, R. Bartolini, and J. Rowland, "Studies of collective effects in SOLEIL and Diamond using the multiparticle tracking codes sbtrack and mbtrack," in *Proceedings of PAC'09, Vancouver, BC, Canada*, 2009, pp. 4637–4639.

[53] T. F. Günzel, U. Iriso, F. Perez, E. Koukovini-Platia, and G. Rumolo, "Analysis of single bunch measurements at the ALBA storage ring," in *Proceedings of IPAC'14, Dresden, Germany*, 2014, pp. 1686–1688.

[54] B. Salvant, "Impedance model of the CERN SPS and aspects of LHC single-bunch stability," PhD thesis 4585, 2010.

[55] R. Bartolini and F. Schmidt, *Sussix: A computer code for frequency analysis of non–linear betatron motion*, CERN-SL-Note-98-017, 1998.

[56] N. Mounet, "The LHC transverse coupled-bunch instability," PhD thesis 5305, EPFL, 2012.

[57] R. Ruth, *Reactive feedback in the two particle model*, CERN-LEP-TH-83-22.

[58] G. Sabbi, *Simulation of coupled-oscillator feedback*, CERN-SL-96-002-AP, 1996.

[59] A. Erdélyi, W. Magnus, F. Oberhettinger, and F. G. Tricomi, *Tables of Integral Transforms*. McGraw-Hill, 1954, vol. 2.

[60] N. Mounet, D. Amorim, and N. Biancacci, `https://github.com/amorimd/CloneDELPHI`, DELPHI repository, 2018.